

## Supporting information

Construction of an intimately riveted Li/garnet interface with ultra-low interfacial resistance for solid-state batteries

Jie Wang,<sup>†ab</sup> Saisai Zhang,<sup>†a</sup> Hailei Zhao,<sup>\*ab</sup> Jintao Liu,<sup>a</sup> Min-An Yang,<sup>a</sup> Zhaolin Li<sup>a</sup>  
and Konrad Świerczek<sup>cd</sup>

<sup>a</sup>School of Materials Science and Engineering, University of Science and Technology  
Beijing, Beijing 100083, China

<sup>b</sup>Beijing Municipal Key Laboratory of New Energy Materials and Technologies,  
Beijing 100083, China

<sup>c</sup>Faculty of Energy and Fuels, Department of Hydrogen Energy, AGH University of  
Krakow, Mickiewicza 30, 30-059 Krakow, Poland

<sup>d</sup>AGH Centre of Energy, AGH University of Krakow, Czarnowiejska 36, 30-054  
Krakow, Poland

\*Corresponding author: hlzhao@ustb.edu.cn.

† These authors contributed equally to this work.

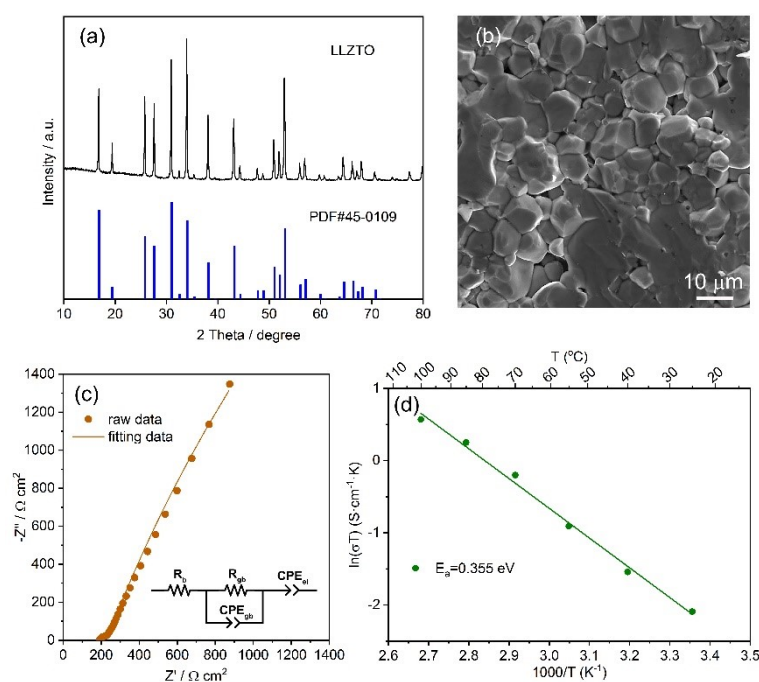


**Fig. S1** (a) XRD pattern of the LLZTO electrolyte. (b) SEM image of the cross-section of the sintered LLZTO pellet. (c) EIS data of LLZTO pellet with Ag blocking electrodes recorded at room temperature. (d) The temperature dependence of the ionic conductivity of LLZTO in the 25-100 °C temperature range, with the calculated activation energy value.

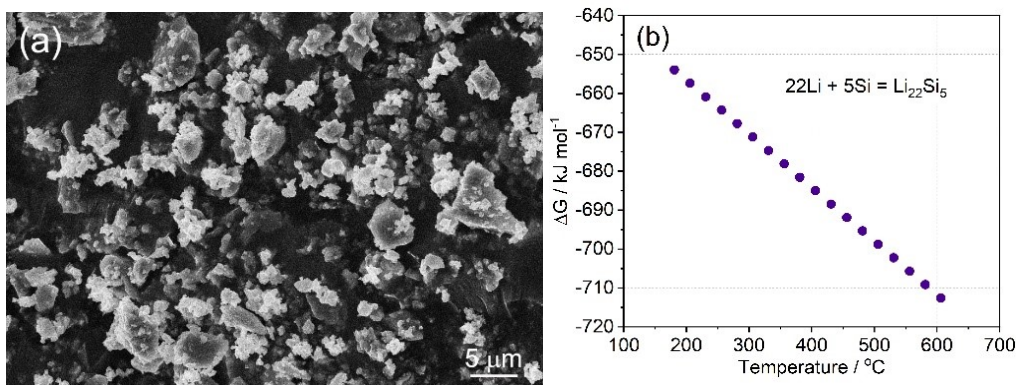


**Fig. S2** (a) SEM image of the commercial Si powder. (b) Gibbs free energy change as a function of temperature for the  $\text{Li}_{22}\text{Si}_5$  formation reaction.

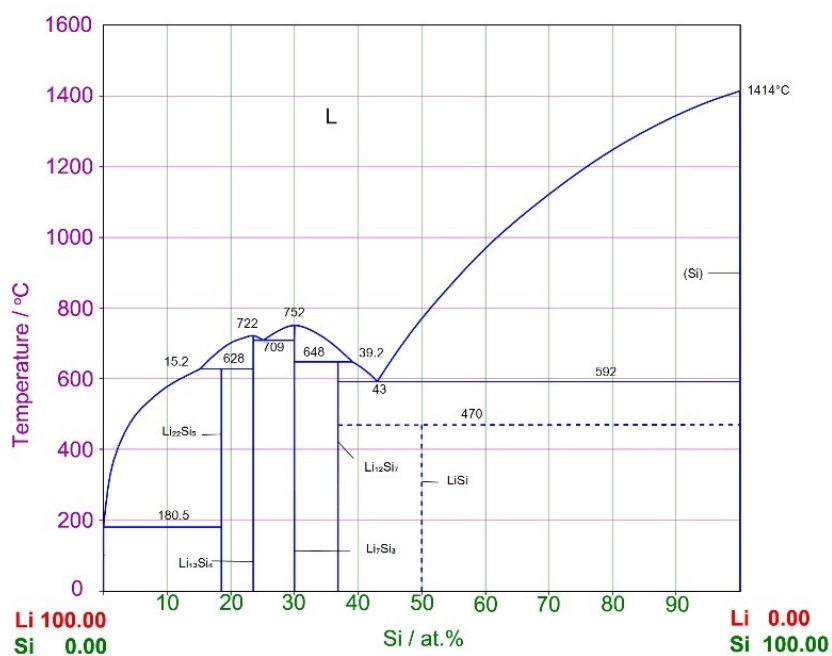


**Fig. S3** The binary phase diagram of Li-Si.

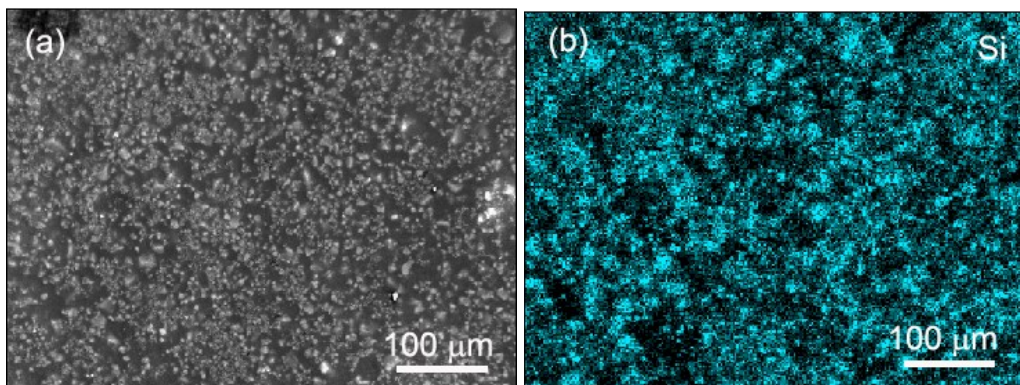


**Fig. S4** (a) Surface SEM and (b) corresponding EDS elemental mapping images of the LSi30 composite.

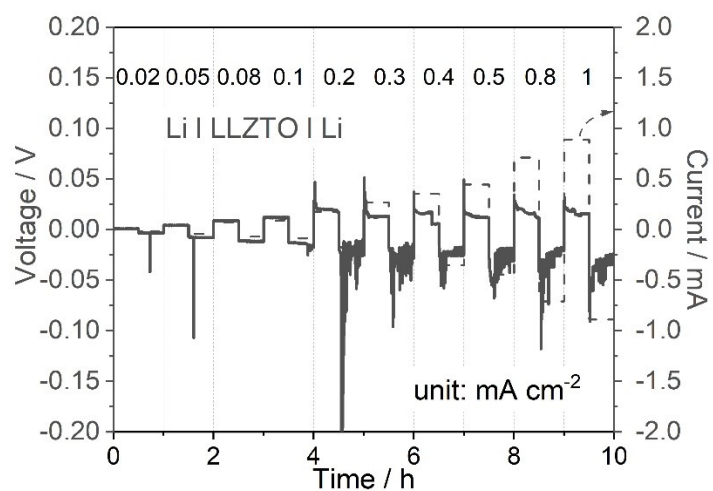


**Fig. S5** CCD of the Li|LLZTO|Li symmetric cell.

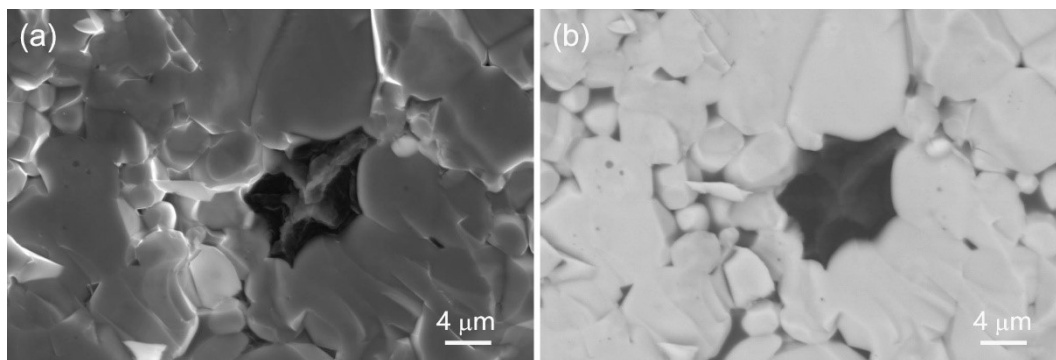


**Fig. S6** Cross-sectional (a) SEM and (b) backscattered electron images of the LLZTO electrolyte from the cycled Li|LLZTO|Li symmetric cell.

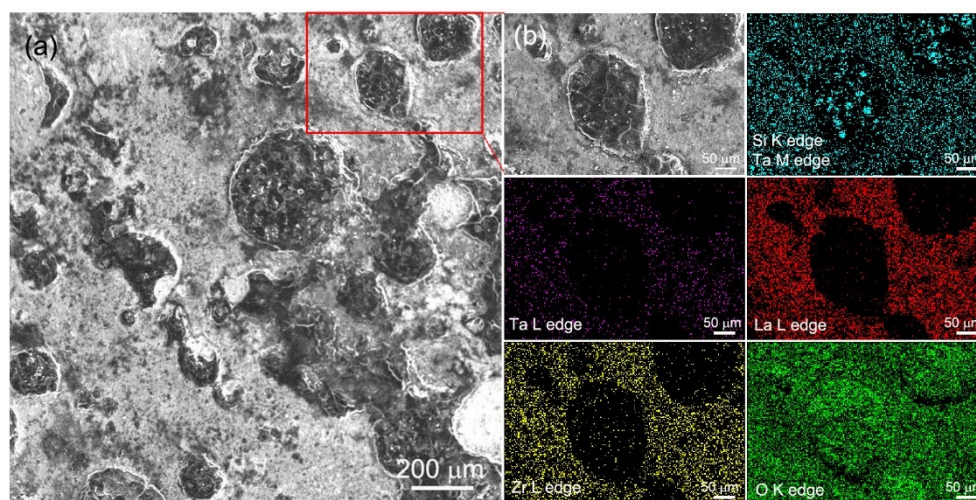


**Fig. S7** (a) Surface SEM and (b) corresponding EDS elemental mapping images of the LLZTO electrolyte after long-term cycling in the LSi15|LLZTO|LSi15 symmetric cell.



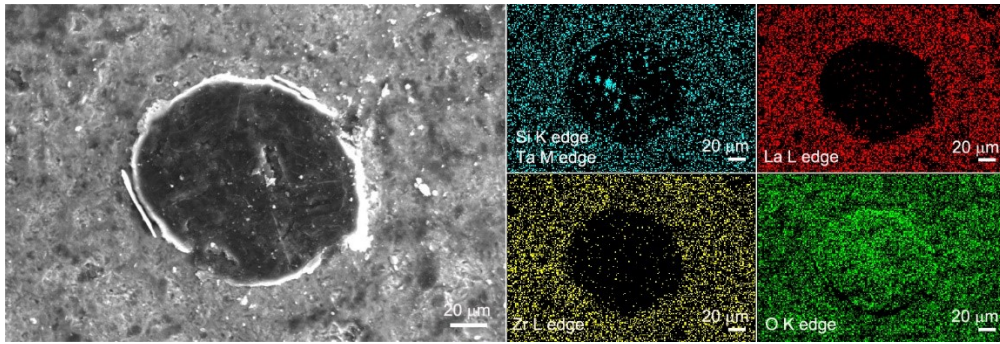


**Fig. S8** SEM and corresponding EDS elemental mapping images of dark spot on the LLZTO surface after long-term cycling in the LSi15|LLZTO|LSi15 symmetric cell.

**Table S1** The detailed calculation results of mutual reaction energy between LLZO and lithiated silicon.

Reactants	Ratio of LLZO	Mutual reaction energy(eV atom <sup>-1</sup> )	Phase equilibria
LLZO+Li <sub>22</sub> Si <sub>5</sub>	100%	0	Li <sub>7</sub> La <sub>3</sub> Zr <sub>2</sub> O <sub>12</sub>
	73.3%	-0.051	Li <sub>2</sub> O,Zr <sub>3</sub> Si <sub>2</sub> ,ZrSi,La <sub>2</sub> O <sub>3</sub>
	66.1%	-0.048	Li <sub>2</sub> O,Zr <sub>3</sub> Si <sub>2</sub> ,Li <sub>2</sub> La <sub>2</sub> Si <sub>3</sub> ,La <sub>2</sub> O <sub>3</sub>
	46.2%	-0.039	Li <sub>2</sub> O,Zr <sub>3</sub> Si <sub>2</sub> ,Li <sub>2</sub> La <sub>2</sub> Si <sub>3</sub> ,Li
	43.5%	-0.037	Li <sub>2</sub> O,ZrSi,Li <sub>2</sub> La <sub>2</sub> Si <sub>3</sub> ,Li
	0%	-0.017	Li <sub>21</sub> Si <sub>5</sub> ,Li
LLZO+Li <sub>21</sub> Si <sub>5</sub>	100%	0	Li <sub>7</sub> La <sub>3</sub> Zr <sub>2</sub> O <sub>12</sub>
	72.4%	-0.046	Li <sub>2</sub> O,Zr <sub>3</sub> Si <sub>2</sub> ,ZrSi,La <sub>2</sub> O <sub>3</sub>
	63.3%	-0.040	Li <sub>2</sub> O,Zr <sub>3</sub> Si <sub>2</sub> ,Li <sub>2</sub> La <sub>2</sub> Si <sub>3</sub> ,La <sub>2</sub> O <sub>3</sub>
	46.2%	-0.030	Li <sub>2</sub> O,Zr <sub>3</sub> Si <sub>2</sub> ,Li <sub>2</sub> La <sub>2</sub> Si <sub>3</sub> ,Li
	43.5%	-0.028	Li <sub>2</sub> O,ZrSi,Li <sub>2</sub> La <sub>2</sub> Si <sub>3</sub> ,Li
	0%	0	Li <sub>21</sub> Si <sub>5</sub>
LLZO+Li	100%	0	Li <sub>7</sub> La <sub>3</sub> Zr <sub>2</sub> O <sub>12</sub>
	12.5%	-0.006	Li <sub>2</sub> O,La <sub>2</sub> O <sub>3</sub> ,Zr <sub>4</sub> O
	0%	0	Li